

Journal of
Applied Remote Sensing

**Spectral response to varying levels of
leaf pigments collected from a degraded
mangrove forest**

Chunhua Zhang
Yali Liu
John M. Kovacs
Francisco Flores-Verdugo
Francisco Flores de Santiago
Ke Chen

Spectral response to varying levels of leaf pigments collected from a degraded mangrove forest

Chunhua Zhang,^a Yali Liu,^b John M. Kovacs,^c Francisco Flores-Verdugo,^d
Francisco Flores de Santiago,^e and Ke Chen^a

^aEast Tennessee State University, Department of Geosciences, Johnson City, Tennessee 37614
zhangc@etsu.edu

^bEast Tennessee State University, Department of Mathematics and Statistics, Johnson City,
Tennessee 37614

^cNipissing University, Department of Geography, North Bay, Ontario, Canada P1B 8L7

^dUniversidad Nacional Autónoma de México, Instituto del Ciencias del Mar y Limnología,
82000 Mazatlán, Sinaloa, México

^eUniversity of Western Ontario, Department of Geography, London, Ontario, Canada N6A 5C2

Abstract. Mangrove forests are being removed or degraded at an alarming rate, even though they play a vital role in the sustainability of tropical coastal communities. Many of these forests are identified as degraded based on observable changes in their leaves (e.g., density, size, color, etc.). Of these, color can be considered one of the most important indicators of degradation because changes in the spectral response may be indicative of changes in the leaf pigment content. In this investigation, hyperspectral laboratory techniques were applied to examine potential relationships between the mangrove leaf spectral response and three leaf pigments: chlorophyll a, chlorophyll b, and total carotenoid content. Using an ASD spectroradiometer, the spectral reflectance of leaf samples were collected from poor condition, dwarf and healthy black (*Avicennia germinans*) and from healthy and poor condition red (*Rhizophora mangle*) mangroves located in a degraded mangrove system of the Mexican Pacific. A subset of 150 representational leaves was then used for pigment content analysis. The results indicate significant relationships between the spectral response and the levels of chlorophyll a, b, and total carotenoid content contained in the leaves. In particular, wavebands at the red edge position were shown to be the best predictors of the pigment contents. The results also indicate that vegetation indices do not necessarily improve the ability to predict these constituents. Finally, the red edge position was found to be significantly different between the healthy and poor condition mangroves ($P = 0$), with the healthy mangroves having longer wavelengths associated with the red edge position. © 2012 Society of Photo-Optical Instrumentation Engineers (SPIE). [DOI: 10.1117/1.JRS.6.063501]

Keywords: mangrove; degradation; hyperspectral remote sensing; pigments; chlorophyll a and b; carotenoids; Mexico.

Paper 11096 received Jun. 1, 2011; revised manuscript received Nov. 17, 2011; accepted for publication Nov. 30, 2011; published online Mar. 12, 2012.

1 Introduction

Mangrove forests are important wetland communities that play a vital role in the ecological and economic sustainability of coastal communities throughout the tropics and subtropics. Economically, they have been identified as an important local renewable resource, a genetic reservoir, and have been shown to be the supportive element of recreational and commercial fisheries.¹ Unfortunately these forested wetlands are being cut or degraded at an alarming rate as the result of various anthropogenic activities, including hydrological modifications, conversion for aquaculture, and deposition of pollutants.¹ As a result, the degradation of mangrove forests has detrimentally impacted the ability of these forests to fix carbon and support local communities

that have depended on these forests for centuries. Consequently, there has been a recent emphasis on developing techniques for monitoring the condition of these coastal wetlands. In particular there have been numerous studies on the use of remotely sensed data to map the distribution and condition of mangrove forests. Wide spectral-band optical and RADAR satellite sensors, such as Landsat, QuickBird, IKONOS, Radarsat and ENVISAT Advanced Synthetic Aperture Radar (ASAR), have been successfully applied to study degraded mangroves.²⁻⁵ These studies show that remote sensing data can be used to map degradation zones based on qualitative measurements, as well as to estimate changes in leaf density (e.g., Leaf Area Index). However, these remote sensing applications do not provide information regarding changes in the chemical components of the leaves, which is critical for our understanding of the physiological changes that occur in these impacted mangrove forests.

Leaf pigments, mainly chlorophyll a (*Chl a*), chlorophyll b (*Chl b*), and carotenoids, are significant compounds responsible for photosynthesis, physiology, and other biological functions. Moreover, variation in the amount of these pigments could be indicative of changes in growth, senescence, disturbance, or stress.⁶ Consequently, pigment contents have been widely examined in studies on vegetation conditions.^{7,8} Methods for estimating pigment contents in remote sensing applications are typically conducted using spectrophotometric analysis. This technique is based on the fact that pigments have various absorption features for different wavebands and, thus, unique combinations of these wavebands can be used to determine pigment contents.^{6,9} Nevertheless, traditional chemical pigment assay analysis can only provide limited point pigment data, i.e., there are always limited pigment data for sample locations.

The availability of a large number of narrow wavelength bands from hyperspectral remote sensing, some of which represent small absorption regions related to pigment content, can make the detection of various pigments possible. Consequently, recent studies have examined the relationship between pigment content in different vegetation types at the leaf level and data obtained using hyperspectral remote sensing techniques in forests,^{10,11} crops, and grass.^{8,12-16} These studies all show significant relationships between the spectral characteristics and leaf pigment content. However, there are overlaps in terms of absorption features for various pigments,⁶ which could hinder the use of a single waveband for measuring pigments. This has led to the introduction of vegetation indices for estimating pigment contents.^{6,17,18} These indices, which make use of two or more bands, have been shown to be particularly useful for estimating *Chl a*. In fact, some studies have reported that many of these indices, including those that integrated only two bands, can provide more accurate pigment estimations and have been shown to be superior to multiple regression models that use five wavelength regions^{6,19} and to partial least square regression models based on the optical and near-infrared spectrum.^{6,20} In addition to the large number of studies on chlorophyll, hyperspectral reflectance data and spectral vegetation indices have also been used to extract carotenoid information.^{11,21} Even a *Chl a*:carotenoid ratio has been reported to be indicative of plant physiology.¹⁸

To examine the relationship between spectral measurements and pigment content, regression analysis has been used by the majority of investigators. However, pseudo-absorption (i.e., a log transformation of reflectance) and derivatives have also been found to increase the correlation between spectral measurements and pigment contents.²¹ Other analytical approaches for estimating pigment content include partial linear square regression,^{22,23} wavelet decomposition,²⁴ and neural networks.¹³

Though a few studies have examined the separation of mangrove species^{25,26} based on hyperspectral data, we found no studies that examined the relationships between the leaf pigment content of mangroves and variation in the spectral responses within individual mangrove species. This absence of data also appears to be lacking for other wetland vegetation communities.²⁷ Therefore, the purpose of this investigation is to determine the feasibility of using hyperspectral products to estimate variation in leaf pigment content for a wide range of mangrove conditions that would be indicative of a degraded state. Specifically, there are three principal objectives: (1) to examine the spectral responses of different mangrove species under various conditions; (2) to study changes in pigment content in mangroves under various conditions; and (3) to investigate the relationship between pigments content and spectral responses.

2 Study Area

The investigated mangrove forest is located just south of the city of Mazatlan in Sinaloa, Mexico (23°09'13" N, 106°19'51" W). This degraded mangrove complex is dominated by black mangrove (*Avicennia germinans*). Based on its height, leaf colors, and distance to water, this mangrove forest can be classified as three dominant conditions: tall (healthy) mangrove, dwarf healthy mangrove, and poor condition mangrove.⁴ Within this mangrove forest, tall healthy black mangroves can be found just inland from a very thin fringe of mixed mangroves that consist primarily of tall healthy red mangrove (*Rhizophora mangle*) with some white mangrove (*Laguncularia racemosa*). These mangroves are generally tall (3 to 5 m, sometimes taller) and support healthy green leaves. Further inland from the tall healthy black mangroves, dwarf black mangroves and poor condition black mangroves can be found. Dwarf black mangroves are generally short (<1 to 2 m) and lack a main stem. However, most dwarf black mangroves have healthy green leaves. Poor condition mangroves, both of the red and black variety, are generally shorter than their tall healthy mangrove counterparts and, moreover, generally support a canopy of stressed leaves. It is not uncommon to see many dead twigs or stems on these mangroves. The majority of the poor condition mangrove stands are located in areas that are relatively far from fresh water sources and, thus, limited by tidal inundations. Changes in hydro-edaphic conditions,²⁸ possibly from road construction and freshwater diversions to support local aquaculture ponds, might be the primary reason for these degraded stands.

3 Methods

3.1 Field Data Collection

Field work was initiated in mid-December 2008 and completed in late January 2009 during the dry season. Leaves from red and black mangroves, representing various conditions, were collected from the top canopy branches with the aid of a hook. Regarding black mangroves, the conditions found included healthy tall black, dwarf black, and poor condition (i.e., degraded) black. Regarding red mangroves, only tall healthy and poor condition samples were located. For many of the tall healthy black and tall healthy red mangroves, the leaves were taken along the tidal channels from a boat using the hook apparatus. Specifically, the third through the fifth leaves from the tip of each branch were clipped so that only mature leaves were collected. In total, 90 samples of black mangrove and 60 samples of red mangrove were gathered, resulting in a sample size of 30 for each of the five stand types examined. All leaves were immediately placed in plastic bags and stored in a cooler at approximately 4°C prior to transportation to the laboratory for spectral reflectance analysis and pigment content determination.

3.2 Spectral Response Measurements

An indoor black house laboratory was set up at the UNAM Instituto del Ciencias del Mar y Limnología Mazatlan Station in order to measure the leaf spectral responses. Canopy reflectance was measured using an ASD FieldSpec® 3 JR spectroradiometer (Analytical Spectral Devices, Inc., USA). The measurement range for this device is 350 to 2500 nm with a spectral resolution of 3 nm from 350 to 1000 nm and 30 nm from 1000 to 2500 nm. The sampling intervals of this equipment are around 1.4 and 2 nm for the visual/near-infrared and short wavelength/infrared regions, respectively. The output spectral data is resampled to 1 nm intervals, so there are, in total, 2150 bands for each spectral measurement. A 50 W halogen light was used as the light source for these indoor measurements. Each reflectance sample was measured based on two layers of mangrove leaves that were stacked facing upwards on a 25-cm diameter matt black plate. The sensor, with a 25-deg viewing angle, was mounted above the plate at a distance of 30 cm. A white reference (spectralon) was used every 5 min in order to calibrate the measurements. For each measurement, the number recorded was based on an average of 15 individual spectral measurements. Four of these average measurements were obtained for each sample by rotating the plate roughly 90 deg each time. These four measurements were then averaged for each sample. The spectral reflectance (R) was first converted to pseudo-absorption ($\log[1/R]$).

The first and second derivatives were then calculated based on the difference in the pseudo-absorption values from two bands with a spectral distance of 2 nm and the range of wavelengths. The position of the red edge was determined using inverted Gaussian fitting using a nonlinear procedure,²⁹ which was followed by derivative analysis. Changes of the red edge position could be used to indicate vegetation conditions and quantify pigment content^{21,30–32} because any decrease in chlorophyll content should decrease the absorption of red light. In addition, five vegetation indices—the Transformed Chlorophyll Absorption in Reflectance Index (TCARI),³³ the Gitelson and Merzylak's Indexes (GMI),³¹ the Vogelmann's Index (VOI),³⁰ the Carter's Stress Index (CSI),⁷ and the Apan's Water Index (AWI)³⁴—were calculated. These indices were selected to identify the spectral relationships of the pigments because they are known to be sensitive to vegetation conditions. TCARI was used to offset potential impacts of the nonphotosynthetic background materials.³² The CSI, GMI, and VOI all utilize the red edge wavebands that are sensitive to plant conditions.

$$\text{TCARI: } 3 \left[(R700 - R670) - 0.2(R700 - R550) \left(\frac{R700}{R670} \right) \right], \quad (1)$$

$$\text{GMI: } \frac{R750}{R700}, \quad (2)$$

$$\text{VOI: } \frac{D715}{D705}, \quad (3)$$

$$\text{CSI: } \frac{R695}{R670}, \quad (4)$$

$$\text{AWI: } \frac{R1660}{R550}, \quad (5)$$

where R and D stand for the reflectance value and the first derivative, respectively, of the waveband identified.

3.3 Leaf Pigment and Water Content Measurements

Following spectral measurements, a number of leaves from each sample were stored in paper bags for transport to a chemical lab where pigment and water content measurements were taken. Leaf pigment data were obtained using the pigment assay method provided by Zarco-Tejada.³⁵ A spectrophotometric analysis was then conducted to determine peak absorption at 646 and 663 nm. The leaf water content of the mangrove leaves was also determined using another portion of the leaf sample that was determined by the difference between the fresh and dry weight. The dry weight was calculated after the leaves had been oven-dried for 48 h at 60°C.

3.4 Statistical Analysis

Analysis of variance (ANOVA) was used to examine the differences in spectral responses between the various mangrove species and their conditions. Specifically, responses were examined based on the mean reflectance at every 10 wavebands and the independent factors included the 215 wavelength regions (average reflectance of every 10-nm wavelength regions), the species, and their interactions. The same analysis was conducted by replacing the species with the mangrove condition. The Pearson's correlation and linear regression were then utilized to examine the relationship between pigment content and spectral response. The coefficient of determination (r^2) was selected as the standard for determining the applicability of wavelengths and vegetation indices for the measurement of pigment content. These three statistical methods—ANOVA, Pearson's correlation, and linear regression—were performed on the red mangrove sample (healthy and poor conditions), the black mangrove sample (healthy, dwarf, and poor conditions) and the entire sample (i.e., pooled). One healthy and two poor condition

red mangrove individual samples were also excluded from the analyses because they were determined to be influential points (i.e., outliers that would have dramatically changed the regression equations). These three samples were considered abnormal samples that simply did not represent the conditions they were originally grouped into. To identify any potential influential points, an initial check was conducted using scatter plots. Using scatter plots, outliers can be easily recognized and, if far enough away from the mean, they can be identified as influential points. Four statistical measures (studentized residual, leverage, Cook's D, and DFFITS) were then calculated to determine whether any outliers with extreme values should be removed for analysis. The conventional cut-off values of 3, $4/n$, $4/n$, and $2/\sqrt{n}$ were used for the studentized residuals, leverage, Cook's D and DFFITS statistics, respectively.

4 Results and Discussion

4.1 Mangrove Pigment Content

As shown in Table 1, the species and condition of the mangrove significantly influence the pigment content. Regarding differences between the species, the red mangrove leaves show a slightly higher overall chlorophyll content ($Chl\ a + Chl\ b$) than the black mangrove leaves (47.8 versus 40.4 mg/m², $P < 0.0001$). Moreover, the mean red mangrove $Chl\ a$ level is also slightly higher than that of the black mangrove ($P = 0.0012$). This discrepancy explains the differences between the species in regards to leaf color. Regarding condition, there are also significant differences in pigment content between healthy and poor condition mangroves. For the red mangrove, the $Chl\ a$ and $Chl\ b$ contents decreased by 17.9 and 5.5 mg/m², respectively ($P < 0.001$ for both variables). Similarly, healthy and poor condition black mangroves showed significant differences in both $Chl\ a$ and $Chl\ b$ contents ($P < 0.0001$). In addition, there were significantly lower $Chl\ a$ (6.2 mg/m², $P < 0.0001$) and $Chl\ b$ (2.98 mg/m², $P < 0.0001$) levels in poor condition black mangroves compared with dwarf black mangroves.

Regarding the total carotenoid content, there was an observed mean decrease of 5.5 mg/m² ($P < 0.0001$) in the poor condition red mangroves and a mean decrease of 2.1 mg/m² ($P < 0.0001$) in poor condition black mangroves compared with respective healthy samples. The ratio of $Chl\ a$ to the total carotenoid content, another indicator of changes in the total carotenoid content, also decreased from 1.8 to 1.4 mg/m² ($P < 0.0001$) and 2.1 to 1.8 mg/m² ($P < 0.0001$) for red and black poor condition mangroves, respectively.

Although the dwarf black mangrove leaf is often visually different from the healthy black mangrove leaf, the results suggest that they are not necessarily different in regard to pigment content. Relatively small differences in $Chl\ a$ and $Chl\ b$ contents were observed between healthy and dwarf black mangroves (Table 1). These differences were determined to be statistically insignificant ($P = 0.130$ and 0.102 , respectively). Regarding the total carotenoid content and $Chl\ a$ /total carotenoid ratio, the P values were significant at 0.039 and 0.024, respectively. In contrast, no significant difference was detected regarding the $Chl\ a$ /total carotenoid ratio ($P = 0.857$) between the dwarf and poor condition black mangrove. Consequently, the results suggest that it is more difficult to distinguish between the dwarf and poor condition black mangroves based simply on pigment content.

4.2 Mangrove Spectral Properties and Leaf Water Content

Mangrove leaves display the typical vegetation curve, with high reflectance in the near-infrared (NIR) and low reflectance in the visible and short-wavelength infrared regions (SWIR) (Fig. 1). Reflectance in the visible region is lower than that in NIR due to chlorophyll absorption and leaf cell wall scattering. The lower reflectance in SWIR regions may reflect changes in the leaf water content. Similar to the pigment contents, there is considerable difference between the two mangrove species in regards to spectral reflectance, particularly in the NIR region. In contrast to healthy black mangrove, the red mangrove has a higher reflectance in NIR and SWIR and lower spectral reflectance in the visible region. The physiological condition also appears to influence the spectral response. In particular, poor condition mangrove has a lower reflectance in NIR and

Table 1 Pigment content of mangroves based on species and condition (Mazatlan, Mexico).

Species	Sample Size	Chlorophyll a (mg/m ²)		Chlorophyll b (mg/m ²)		Total carotenoids (mg/m ²)		Chlorophyll a/carotenoids	
		Mean ± standard error	Range	Mean ± standard error	Range	Mean ± standard error	Range	Mean ± standard error	Range
All mangroves	147	32.7 ± 0.7	38.1	10.6 ± 0.3	16.6	18.5 ± 0.3	15.2	1.8 ± 0.03	1.6
<i>Rhizophora mangle</i>	57	35.4 ± 1.4	38.1	12.4 ± 0.5	15.1	21.6 ± 0.5	14.8	1.6 ± 0.04	1.3
Healthy	29	44.2 ± 1.3	23.4	15.0 ± 0.5	10.9	24.3 ± 0.4	7.7	1.8 ± 0.05	1.0
Poor condition	28	26.3 ± 0.7	14.5	9.6 ± 0.3	6.6	18.8 ± 0.5	10.7	1.4 ± 0.03	0.8
<i>Avicennia germinans</i>	90	31.0 ± 0.6	24.5	9.4 ± 0.3	10.4	16.5 ± 0.2	9.5	1.9 ± 0.03	1.3
Healthy	30	34.3 ± 1.0	23.8	11.0 ± 0.4	8.0	16.6 ± 0.2	5.4	2.1 ± 0.06	1.3
Dwarf	30	32.5 ± 0.6	12.1	10.1 ± 0.4	8.1	18.3 ± 0.3	6.7	1.8 ± 0.05	1.0
Poor condition	30	26.3 ± 0.6	14.0	7.2 ± 0.2	4.9	14.5 ± 0.3	4.2	1.8 ± 0.02	0.5

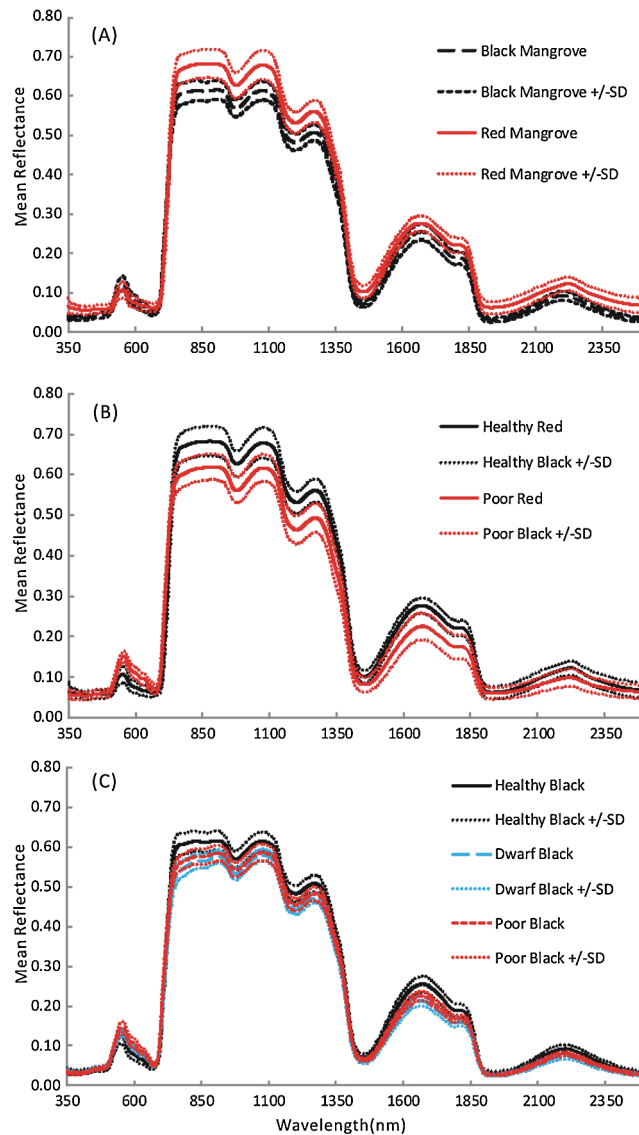


Fig. 1 Spectral curves of healthy mangroves (a), healthy and poor condition *Rhizophora mangle* (b), and healthy, dwarf, and poor condition *Avicennia germinans* (c) leaves. While reflectance in the visible light region is mainly influenced by leaf pigments, strong reflectivity in NIR can be caused by cell structure (cell wall scattering). Water content is the main influencer on shortwave infrared, and there are five main water absorption regions centered at 960, 1190, 1430, 1910, and 2700 nm (not shown).

higher reflectance in the visible wavelengths and SWIR. The higher reflectance in the visible region explains the yellowish leaf color (i.e., chlorosis) of the degraded mangroves. The reflectance of NIR is principally controlled by the walls of the spongy mesophyll cells, with healthier leaves tending to have stronger reflectance in NIR as they reflect excessive amount of incoming energy in this region of the electromagnetic spectrum. In contrast, stressed leaves will have lower reflectance due to cell structure changes. The leaf water content is the main determinant of reflectance in the SWIR region. A higher leaf water content should theoretically increase absorption in SWIR and, thus, contribute to a decrease in reflectance. The higher reflectance of healthier mangroves in SWIR was unexpected given that one would assume that the healthier mangrove leaves should contain a higher water content. For the red mangroves, the water content actually increased from 64.7% in healthy leaves to 69.3% in poor condition leaves ($P < 0.001$). Conversely, for black mangroves, both the dwarf (61.5%) and stressed black (62.0%) mangroves had lower water contents than healthy black mangroves (68.4%). The

water content of stressed black mangroves was slightly higher than that of dwarf black mangroves, though no significant differences were observed ($P = 0.536$). However, reflectance curves reported in a recent study²⁶ also showed decreased reflectance in the SWIR region for what are, presumably, degraded mangrove leaves. Consequently, this contradictory situation might signify other physiological factors, unique to mangrove leaves, which contribute to the spectral variation in this region of the electromagnetic spectrum. It is also worth noting that the spectral reflectance of the dwarf black mangrove is lower than that of the poor condition black mangrove in NIR and SWIR. This is contradictory to the higher reflectance in the visual light wavelength regions, where lower reflectance was observed for dwarf black mangrove. It has been reported that stressed mangroves shed leaves less often than healthy mangroves and stressed mangrove leaves are generally smaller and thicker.³⁶ These findings might explain the variations in SWIR and indicate that further work should be conducted to explore the impact of environmental degradation on mangrove leaf structure. In addition to all the differences, there are significant differences in the spectral responses measured in mangroves under various conditions ($P < 0.0001$).

4.3 Relationship Between Spectral Response and Pigment Content

Although the water content in fresh leaves may decrease absorption in NIR and SWIR,³⁷ the results indicate significant relationships between pigment content and reflectance (or pseudo-absorbance) for a variety of wavebands. Two wavelength regions in particular, the green and the red edge, demonstrated strong to very strong correlations with *Chl a* and *Chl a* + *Chl b* (Fig. 2). For *Chl a*, *Chl b*, carotenoids, and *Chl a* + *Chl b*, strong to very strong correlations were observed, mainly in the green light and red edge position, with the maximum correlation coefficients appearing around 560 nm and 705 nm, respectively. Because the main factor that influences spectral reflectance in the visible light portion of plant leaves is the pigment concentration^{11,30} this result is what would be expected. In contrast, no strong correlations between reflectance in the red and blue light regions and pigment contents of the mangrove leaves were demonstrated. This would suggest that these wavebands are not sensitive to pigment content variation.¹¹ Regarding NIR and SWIR, only weak to moderate correlations were demonstrated. In general, the sum of *Chl a* and *Chl b* depicted extremely strong correlations with reflectance in the visible light region of all mangrove samples ($r = -0.83$, $P < 0.001$). However, some correlation coefficients for chlorophylls at the species level (for red mangrove)

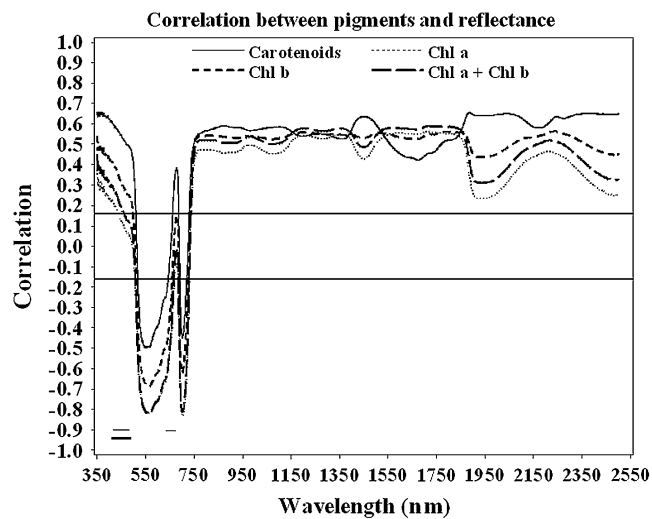


Fig. 2 Correlogram of leaf *Chl a* content and pseudo-absorption of all mangrove samples. Two horizontal lines indicate the 0.05 significance level. The two thin line segments indicate strong absorption of *Chl a* and *Chl b*, whereas the thick line segment indicates the strong absorptive region for total carotenoids.

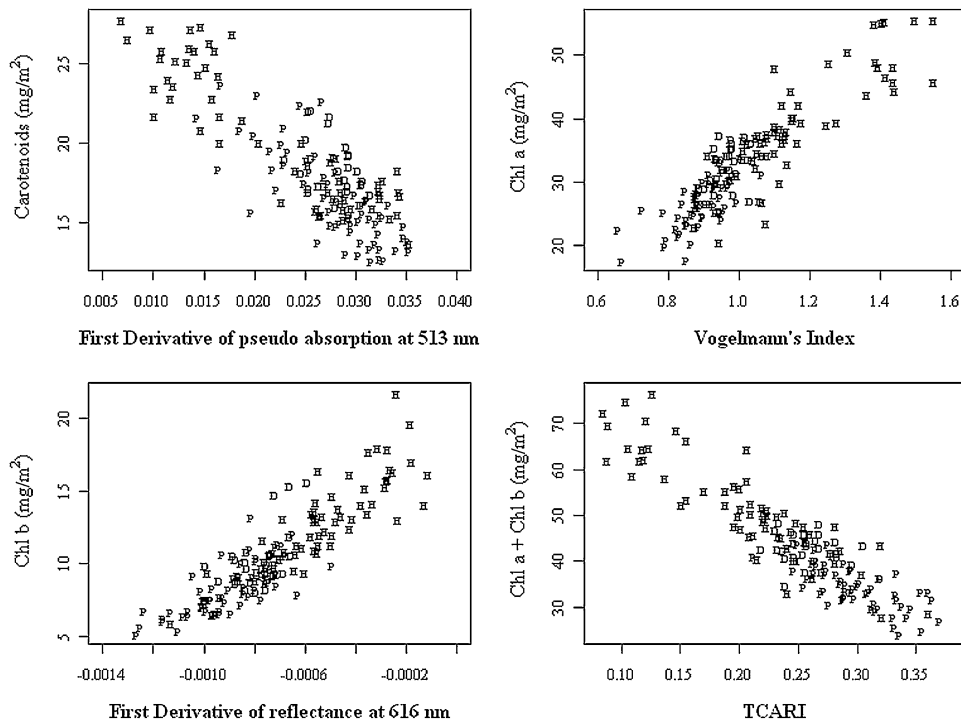


Fig. 3 Scatterplots of pigment versus derivatives (or vegetation index) for *Avicennia germinans* leaves. D, H, and P stand for dwarf, healthy, and poor condition, respectively.

were over -0.9 (data not shown). In contrast, correlations between total carotenoid content and spectral reflectance were weak to moderate.

Applications of linear regression were used to examine the utility of selected wavebands for measuring pigment content because the data for the mangrove leaves (Fig. 3) were consistent with the general trend for linear relationships between chlorophyll content and spectral data. The results of the analyses (Table 2) suggest that spectral information from single bands around the red edge (690 to 750 nm) could be utilized to measure pigment content in these leaves. In particular, wavebands around 693 and 713 nm have a higher frequency of selection (Table 2) and, therefore, were selected as the most useful bands for pigment content determination. Models based on derivatives show relatively large coefficients of determination (r^2) (Table 2). In fact, the majority (77.7%) of the r^2 values depict values >0.6 , which would indicate that hyperspectral remote sensing could be an efficient tool for pigment determination in these wetlands.

Regarding species differences, most of the r^2 values for the black mangrove were lower than those of the red mangrove (e.g., *Chl a* and *Chl a + Chl b*). This result may be explained by the degree of degradation between the two species, with the poor condition black mangrove sample showing less degradation compared with poor condition red mangrove sample. Therefore, the larger contrast of the red mangrove would highly influence the linear relationships between the spectral responses and the chemical components. There are other wavebands within SWIR that are not listed in Table 2 that also show a high efficiency of prediction (e.g., 2032 nm for red mangrove, $r^2 = 0.611$). These relationships might be indirectly caused by nitrogen absorption because 2060 nm is a known nitrogen-absorption region.³⁸ In general, r^2 values for *Chl b* are lower than for those of *Chl a*, which may simply be the result of lower *Chl b* content within the leaves. In addition, many of the wavebands selected in Table 2 are in red wavelength region where absorption is dominated by *Chl a*.¹¹

In addition to the chlorophyll content, strong relationships were also demonstrated between the total carotenoid content and the spectral data, which was not expected given that previous studies have not reported such relationships.²¹ The results of this study (Table 2) indicate strong correlations for mangroves, particularly for the pooled (i.e., all) mangrove data. The waveband of 690 nm was negatively related to carotenoid content. Both wavebands 512 and 513 nm, which are unknown to be within the strongest absorption region of carotenoids, also showed

Table 2 Relationships between pigments and spectral data (*black* = *A.germinans*; *red* = *R.mangle*).

Biochemical attributes	Mangroves	Independent Variable	Wavebands (nm)	Models	r^2
<i>Chl a</i>	pooled	First Derivative ²	694	55.766 – 3087.351x	0.785
	black	First Derivative ¹	744	–4.615 – 3953.174x	0.574
	red	Second Derivative ¹	749	–11.503 + 71659.402x	0.883
<i>Chl b</i>	pooled	First Derivative ²	616	18.730 + 11304.282x	0.768
	black	First Derivative ²	619	18.057 + 14061.670x	0.723
	red	Second Derivative ²	713	11.738 + 10016.272x	0.772
<i>Chl a</i> + <i>Chl b</i>	pooled	First Derivative ²	693	71.460 – 4372.993x	0.806
	black	First Derivative ²	693	71.158 – 4467.075x	0.692
	red	Second Derivative ²	713	45.142 + 42662.929x	0.884
Total carotenoids	pooled	First Derivative ¹	513	–30.132 + 459.163x	0.726
	black	Second Derivative ²	690	26.553 – 9551.332x	0.540
	red	First Derivative ¹	512	–29.948 + 473.222x	0.675
<i>Chl a</i> /carotenoids	pooled	Second Derivative ²	722	14.565 + 15317.518x	0.457
	black	First Derivative ¹	715	–3.418 – 308.460x	0.474
	red	Second Derivative ²	737	7.701 – 3873.414x	0.681

¹Derivatives of pseudo-absorption.²Derivatives of reflectance.

strong correlations. This indicates that the wavelength region around 510 nm could be very useful for carotenoids determination in mangroves. Although the *Chl a*/carotenoid ratio has been reported as a good indicator of the carotenoid content,²¹ in this study this parameter was not found to be superior to the total carotenoid content for predicting carotenoid contents. However, the r^2 values for total carotenoid content and *Chl a*/carotenoid ratio were quite similar. The relatively large range of observed r^2 values (0.46 to 0.68) suggests the accurate mapping of the spatial distribution of the total carotenoid content in mangroves is possible with these data. However, it is recommended that more experiments be conducted to verify this claim.

4.4 Vegetation Indices and Pigment Measurements

Previous studies have suggested that vegetation indices can be very useful for extracting pigment information.³⁹ However, in this investigation, these vegetation indices did not increase the ability of prediction. The r^2 values of many of the calculated vegetation indices (Table 3) were smaller than for those of single wavebands (Table 2). For example, the VOI demonstrated the highest

Table 3 Relationships between vegetation indices and pigment content (*red* = *R.mangle*; *black* = *A.germinans*).

Dependent	Mangroves	Models	r^2
<i>Chl a</i>	Pooled	–10.262 + 42.303 VOI	0.788
	Black	–3.338 + 9.239 VOI	0.622
	Red	63.048 – 124.162 TCARI	0.876
<i>Chl b</i>	Pooled	21.330 – 42.845 TCARI	0.719
	Black	22.502 – 48.517 TCARI	0.667
	Red	3.385 + 4.324 AWI	0.709
<i>Chl a</i> + <i>Chl b</i>	Pooled	82.542 – 156.289 TCARI	0.818
	Black	–5.834 + 13.565 VOI	0.721
	Red	83.520 – 160.629 TCARI	0.867
Total carotenoids	Pooled	38.062 – 10.352 CSI	0.700
	Black	25.435 – 33.285 TCARI	0.400
	Red	6.472 + –1.519 CSI	0.426
<i>Chl a</i> /carotenoids	Pooled	8.841 + 2.128 AWI	0.285
	Black	5.343 + 2.199 GMI	0.475
	Red	6.914 + 2.421 AWI	0.650

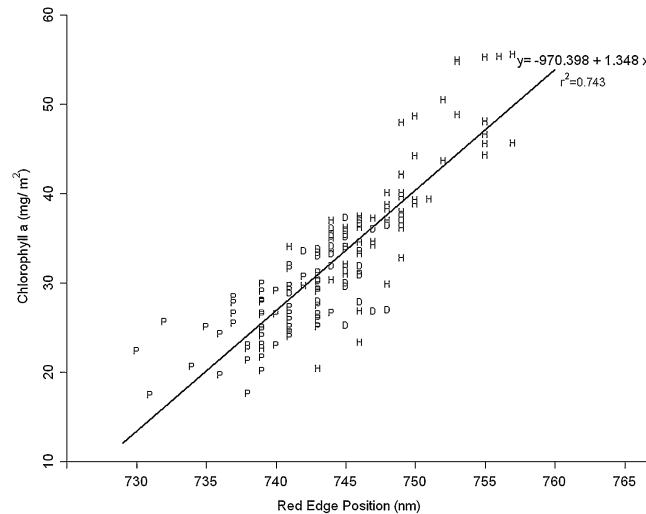


Fig. 4 Scatter plot of *Chl a* and the red edge position.

potential for the prediction of *Chl a* with an r^2 value of 0.788, which is only 0.003 higher than that of waveband 694 nm. Only a few indices (e.g., TCARI) were able to slightly enhance the r^2 value (Table 3). TCARI is also the index that has the highest frequency for chlorophyll content prediction (Table 3).

4.5 Red Edge Position and Pigment Content

Similar to others studies,²¹ the results of this study indicate roughly positive relationships between red edge positions and chlorophyll concentrations. Healthy red mangroves have longer red edge positions than those of tall healthy black mangroves (751 and 746 nm respectively, $P = 0.001$). The red edge positions of the dwarf black and the tall black mangrove are relatively close (744 and 746 nm, respectively, $P = 0.017$), which is expected since both are in healthy conditions. In contrast, the poor condition red mangroves' red edge position was found to be around 740 nm. Fairly strong r^2 values were calculated for the red edge position and the *Chl a* content (Fig. 4). A linear regression model, fitted to examine the relationship of all mangrove samples, indicated a general trend of longer red edge wavelengths for healthy mangroves and shorter red edge positions for poor condition mangroves. The dwarf mangroves' red edge positions were found between those of the healthy and the poor condition mangrove with some overlap between these two conditions. Consequently, the red edge position could be a good indicator of health. Four tall healthy black samples showed small red edge positions (739 to 742 nm). Interestingly, these samples also had lower than average water contents. The red edge position shift has also been shown to be related to water content and stress, with a slight loss in water content shifting the red edge to the longer wavelength region and with even more water loss, shifting it to the short wavelength regions.⁴⁰ Consequently, the water content may have influenced the red edge position of these samples.

5 Conclusions

The results of this investigation indicate that hyperspectral techniques can be used to study and monitor changes in pigments that results from the degradation of a mangrove forest. The data indicate that there are significant differences in *Chl a*, *Chl b*, and total carotenoid contents for different mangrove species and mangrove conditions. Specifically, red mangrove leaves have higher chlorophyll and carotenoids contents than black mangroves. Moreover, healthy mangroves contain higher pigment contents than poor condition mangroves, and all of these aforementioned differences are also present in the spectral responses of different mangrove species. Generally, red healthy mangroves have higher reflectance of NIR and SWIR and lower

reflectance of the visible region in comparison to black healthy mangroves. There are also strong correlations between pigment content and spectral response to green light and the red edge position (680 to 750 nm). Based on these wavebands, the relationships between wavebands and pigments have been examined using linear regression for all mangroves, black mangrove, and red mangrove. Values of r^2 from these models varied from 0.457 to 0.87, with most values around 0.65 to 0.8. Comparatively, the vegetation indices only show a slightly stronger ability to predict chlorophyll contents. Of these, TCARI and VOI were found to be the best vegetation indices for pigment content prediction. An examination of red edge position showed that there is a positive correlation between this parameter and *Chl a*, and that these mangroves could be classified into two contrasting groups based on red edge positions.

Although the approach taken in this study did provide pertinent information, there are some issues to be considered if one is to conduct a similar investigation. For example, the storage and transportation of leaves should be done in a timely fashion. Fortunately, in this study, the laboratory facilities were close to the field site. Moreover, given the responses of the poor condition mangroves, it is also suggested that further examination of this population be conducted by including a larger sample and by examining other leaf constituents (e.g., nitrogen) in relation to spectral data. Issues can also arise if one is to scale up the relationships between leaf pigment contents and spectral responses to large scale mapping using spaceborne remote sensing data. Further studies should be conducted to examine the impacts of canopy structure characteristics, such as leaf angle distribution, leaf size, crown shape, canopy height, canopy closure, and background information, on the spectral response.

Acknowledgments

This research was supported by grants awarded to Chunhua Zhang from the East Tennessee State University Research Develop Committee (Grant #RD0096) and to John M. Kovacs from the Natural Sciences and Engineering Research Council of Canada (Grant #249496-06).

References

1. B. B. Walters et al., "Ethnobiology, socio-economics and management of mangrove forests: a review," *Aquat. Bot.* **89**(2), 220–236 (2008), <http://dx.doi.org/10.1016/j.aquabot.2008.02.009>.
2. E. P. Green et al., "Remote sensing techniques for mangrove mapping," *Int. J. Rem. Sens.* **19**(5), 935–956 (1998), <http://dx.doi.org/10.1080/014311698215801>.
3. J. M. Kovacs, J. Wang, and F. Flores-Verdugo, "Mapping mangrove leaf area index at the species level using IKONOS and LAI-2000 sensors for the Agua Brava Lagoon, Mexican Pacific," *Estuar. Coast. Shelf Sci.* **62**(1–2), 377–384 (2005), <http://dx.doi.org/10.1016/j.ecss.2004.09.027>.
4. J. M. Kovacs et al., "The use of multipolarized spaceborne SAR backscatter for monitoring the health of a degraded mangrove forest," *J. Coastal Res.* **24**(2), 248–254 (2008), <http://dx.doi.org/10.2112/06-0660.1>.
5. J. M. Kovacs et al., "Evaluating the condition of a mangrove forest of the Mexican Pacific based on an estimated leaf area index mapping approach," *Environ. Monit. Assess.* **157**(1–4), 137–149 (2009), <http://dx.doi.org/10.1007/s10661-008-0523-z>.
6. G. A. Blackburn, "Hyperspectral remote sensing of plant pigments," *J. Exp. Bot.* **58**(4), 855–867 (2007), <http://dx.doi.org/10.1093/jxb/erl123>.
7. G. A. Carter and R. L. Miller, "Early detection of plant stress by digital imaging within narrow stress-sensitive wavebands," *Rem. Sens. Environ.* **50**(3), 295–302 (1994), [http://dx.doi.org/10.1016/0034-4257\(94\)90079-5](http://dx.doi.org/10.1016/0034-4257(94)90079-5).
8. J. Li and J. Jiang et al., "Using hyperspectral indices to estimate foliar chlorophyll a concentrations of winter wheat under yellow rust stress," *New Zealand J. Agric. Res.* **50**(5), 1031–1036 (2007), <http://dx.doi.org/10.1080/00288230709510382>.
9. H. K. Lichtenthaler, "Chlorophylls and carotenoids: pigments of photosynthetic membranes," *Methods Enzymol.* **148**(2), 350–382 (1987), [http://dx.doi.org/10.1016/0076-6879\(87\)48036-1](http://dx.doi.org/10.1016/0076-6879(87)48036-1).

10. G. A. Blackburn, "Relationships between spectral reflectance and pigment concentrations in stacks of broadleaves," *Remote Sens. Environ.* **70**(2), 224–237 (1999), [http://dx.doi.org/10.1016/S0034-4257\(99\)00048-6](http://dx.doi.org/10.1016/S0034-4257(99)00048-6).
11. B. Datt, "Remote sensing of chlorophyll a, chlorophyll b, chlorophyll a+b and total carotenoid content in eucalyptus leaves," *Remote Sens. Environ.* **66**(2), 111–121 (1998), [http://dx.doi.org/10.1016/S0034-4257\(98\)00046-7](http://dx.doi.org/10.1016/S0034-4257(98)00046-7).
12. J. L. Boggs et al., "Relationship between hyperspectral reflectance, soil nitrate-nitrogen, cotton leaf chlorophyll, and cotton yield: a step toward precision agriculture," *J. Sustain. Agric.* **22**(3), 5–16 (2003), http://dx.doi.org/10.1300/J064v22n03_03.
13. L. Chen et al., "Comparison between backpropagation neural network and regression models for estimation of pigment content in rice leaves and panicles using hyperspectral data," *Int. J. Remote Sens.* **28**(16), 3457–3478 (2007), <http://dx.doi.org/10.1080/01431160601024242>.
14. C. S. T. Daughtry et al., "Estimating corn leaf chlorophyll concentration from leaf and canopy reflectance," *Remote Sens. Environ.* **74**(2), 229–239 (2000), [http://dx.doi.org/10.1016/S0034-4257\(00\)00113-9](http://dx.doi.org/10.1016/S0034-4257(00)00113-9).
15. S. Ge et al., "Canopy assessment of biochemical features by ground-based hyperspectral data for an invasive species, giant reed (*Arundo donax*)," *Environ. Monitor. Assess.* **147**(1–3), 271–278 (2008), <http://dx.doi.org/10.1007/s10661-007-0119-z>.
16. S. D. Tumbo, D. G. Wagner, and P. H. Heinemann, "Hyperspectral characteristics of corn plants under different chlorophyll levels," *Trans. ASAE* **45**, 815–823 (2008).
17. E. W. Chappelle, M. S. Kim, and J. E. McMurtrey, "Ratio analysis of reflectance spectra (PARS): an algorithm for the remote estimation of the concentration of chlorophyll A, chlorophyll B and the carotenoids in soybean leaves," *Remote Sens. Environ.* **39**(3), 239–247 (1992), [http://dx.doi.org/10.1016/0034-4257\(92\)90089-3](http://dx.doi.org/10.1016/0034-4257(92)90089-3).
18. J. Penuelas, F. Baret, and I. Filella, "Semi-empirical indices to assess carotenoids/chlorophyll a ratio from leaf spectral reflectance," *Photosynthetica* **31**, 221–230 (1995).
19. P. K. Goel et al., "Estimation of crop biophysical parameters through airborne and field hyperspectral remote sensing," *Trans. ASAE* **46**, 1235–1246 (2003).
20. P. M. Hansen and J. K. Schjoerring, "Reflectance measurement of canopy biomass and nitrogen status in wheat crops using normalized difference vegetation indices and partial least squares regression," *Remote Sens. Environ.* **86**(4), 542–553 (2003), [http://dx.doi.org/10.1016/S0034-4257\(03\)00131-7](http://dx.doi.org/10.1016/S0034-4257(03)00131-7).
21. G. A. Blackburn, "Quantifying chlorophylls and carotenoids at leaf and canopy scale: an evaluation of some hyperspectral approaches," *Remote Sens. Environ.* **66**(3), 273–285 (1998), [http://dx.doi.org/10.1016/S0034-4257\(98\)00059-5](http://dx.doi.org/10.1016/S0034-4257(98)00059-5).
22. K. Bolster, M. E. Martin, and J. D. Aber, "Determination of carbon fraction and nitrogen concentration in tree foliage by near infrared reflectance: a comparison of statistical methods," *Can. J. Forest Res.* **26**(4), 590–600 (1996), <http://dx.doi.org/10.1139/x26-068>.
23. Z. Huang et al., "Estimating foliage nitrogen concentration from HYMAP data using continuum removal analysis," *Remote Sens. Environ.* **93**(1–2), 18–29 (2004), <http://dx.doi.org/10.1016/j.rse.2004.06.008>.
24. G. A. Blackburn, "Wavelet decomposition of hyperspectral data: a novel approach to quantifying pigment concentrations in vegetation," *Int. J. Remote Sens.* **28**(12), 2831–2855 (2007), <http://dx.doi.org/10.1080/01431160600928625>.
25. C. Vaiphasa et al., "Tropical mangrove species discrimination using hyperspectral data: a laboratory study," *Estuar. Coast. Shelf Sci.* **65**(1–2), 371–379 (2005), <http://dx.doi.org/10.1016/j.ecss.2005.06.014>.
26. L. Wang and W. P. Sousa, "Distinguishing mangrove species with laboratory measurements of hyperspectral leaf reflectance," *Int. J. Remote Sens.* **30**(5), 1267–1281 (2009), <http://dx.doi.org/10.1080/01431160802474014>.
27. E. Adam, O. Mutanga, and D. Rugege, "Multispectral and hyperspectral remote sensing for identification and mapping of wetland vegetation: a review," *Wetlands Ecol. Manage.* **18**(3), 281–296 (2009), <http://dx.doi.org/10.1007/s11273-009-9169-z>.

28. G. Naidoo, "Factors contributing to dwarfing in the mangrove *Avicennia marin*," *Annals Bot.* **97**(6), 1095–1101 (2006), <http://dx.doi.org/10.1093/aob/mcl064>.
29. G. F. Bonham-Carter, "Numerical procedures and computer program for fitting an inverted Gaussian model to vegetation reflectance data," *Comput Geosci.* **14**(3), 339–356 (1988), [http://dx.doi.org/10.1016/0098-3004\(88\)90065-9](http://dx.doi.org/10.1016/0098-3004(88)90065-9).
30. J. E. Vogelmann, B. N. Rock, and D. M. Moss, "Red edge spectral measurements from sugar maple leaves," *Int. J. Remote Sens.* **14**(8), 1563–1575 (1993), <http://dx.doi.org/10.1080/01431169308953986>.
31. A. A. Gitelson, M. N. Merzylak, and H. K. Lichtenthaler, "Detection of red edge position and chlorophyll content by reflectance measurements near 700 nm," *J. Plant Physiol.* **148**, 501–508 (1996), [http://dx.doi.org/10.1016/S0176-1617\(96\)80285-9](http://dx.doi.org/10.1016/S0176-1617(96)80285-9).
32. A. Pinar and P. J. Curran, "Grass chlorophyll and the reflectance red edge," *Int. J. Remote Sens.* **17**(2), 351–357 (1996), <http://dx.doi.org/10.1080/01431169608949010>.
33. D. Haboudance et al., "Integrated narrow band vegetation indices for prediction of crop chlorophyll content for application to precision agriculture," *Remote Sens. Environ.* **81**(2–3), 416–426 (2002), [http://dx.doi.org/10.1016/S0034-4257\(02\)00018-4](http://dx.doi.org/10.1016/S0034-4257(02)00018-4).
34. A. Apan et al., "Detecting sugarcane 'orange rust' disease using EO-1 Hyperion hyperspectral imagery," *Int. J. Remote Sens.* **25**(2), 489–498 (2004), <http://dx.doi.org/10.1080/01431160310001618031>.
35. P. J. Zarco-Tejada et al., "Assessing vineyard condition with hyperspectral indices: leaf and canopy reflectance simulation in a row-structured discontinuous canopy," *Remote Sens. Environ.* **99**(3), 271–287 (2005), <http://dx.doi.org/10.1016/j.rse.2005.09.002>.
36. A. E. Lugo et al., "Ecophysiology of a mangrove forest in Jobos Bay, Puerto Rico," *Caribbean J. Sci.* **43**(2), 200–219 (2007), <http://dx.doi.org/10.1080/01431169008955129>.
37. C. D. Elvidge, "Visible and near infrared reflectance characteristics of dry plant materials," *Int. J. Remote Sens.* **11**(10), 1775–1795 (1990), <http://dx.doi.org/10.1080/01431169008955129>.
38. P. J. Curran, "Remote sensing of foliar chemistry," *Remote Sens. Environ.* **30**(3), 271–278 (2008), [http://dx.doi.org/10.1016/0034-4257\(89\)90069-2](http://dx.doi.org/10.1016/0034-4257(89)90069-2).
39. C. Wu, Z. Niu, Q. Tang, and W. Huang, "Estimating chlorophyll content from hyperspectral vegetation indices: modeling and validation," *Agric. Forest Meteorol.* **148**(8–9), 1230–1241 (2008), <http://dx.doi.org/10.1016/j.agrformet.2008.03.005>.
40. D. N. H. Horler, M. Dockray, and J. Barber, "The red edge of plant reflectance," *Int. J. Remote Sens.* **4**(2), 273–288 (1983), <http://dx.doi.org/10.1080/01431168308948546>.

Biographies and photographs of the authors not available.